

## 2. ELECTROCHEMISTRY

About 230 years ago, an anatomist, Luigi Galvani, accidentally touched his steel scalpel to a brass hook holding a frog leg in place. Upon contact, the frog leg twitched and the first observation of electrochemistry was made in a laboratory. Galvani chalked it up to biological processes that he termed “animal electricity.” Meanwhile, Alessandro Volta replicated his experiments and contended that the electricity was generated by the two dissimilar metals, not from some process inside the animal. He demonstrated his theory by building voltaic piles, essentially alternating metal plates sandwiched by cardboard soaked in salt water. Both were right. Galvani’s approach gave birth to neurophysiology, while Volta’s approach made him the father of modern day electrochemistry (51).

The voltaic pile was the first form of continuous electric current, a necessity for the development of electrochemistry and most modern technologies. A string of scientists picked up Volta’s work, and the field of electrochemistry has grown to include applications in almost every field. To describe the behavior of ions in electrochemical cells, electrochemistry blends three fundamental subjects: (1) thermodynamics, (2) reaction kinetics, and (3) mass transport. From these fundamental matters, all electrochemical relations and techniques are derived. To facilitate the discussion of the fundamentals matters in the context of electrochemistry, some general terms and concepts of electrochemistry need to be introduced.

## 2.1. General Overview

Electrochemical studies are usually carried out in an electrochemical cell. An electrochemical cell consists of four main components: a power supply, an anode, a cathode, and an electrolyte. The power supply drives the reaction. Material is oxidized at the anode and reduced at the cathode. The electrolyte serves as a conducting medium to allow the flow of ions in the cell. In electroanalytical work, the power supply is replaced by a potentiostat which can manipulate and measure the potential and/or current at an electrode. This electrode is called the working electrode (WE) and can function as either the anode or cathode depending upon the conditions imposed. A counter electrode (CE) serves as the other electrode to close the electrochemical circuit. An additional electrode called a reference electrode (RE) is commonly used in electroanalytical work. The RE provides a stable potential to which the WE can be compared or referenced. In molten LiCl-KCl eutectic, the RE is commonly based on the silver-silver chloride (Ag/AgCl) redox couple or a chlorine ion and gas  $[\text{Cl}^-/\text{Cl}_2 (1 \text{ atm})]$  redox couple.

Typically, electroanalytical techniques are interested in the reaction of a certain species, called an analyte, that liberates (oxidation) or consumes (reduction) electrons at the WE. These reactions are generally represented by the following reaction and written so that the forward reaction is the reduction reaction.



In molten LiCl-KCl eutectic, the analyte is usually a monoatomic metal ion, which applied to (2.1) results in the following equation



Of primary concern, in this work, is the reduction of metal ions to metal in the zero

valance state or the reverse reaction of oxidation from metal to a metal ion. Applying the assumption of zero valance state to (2.2) (i.e.,  $p = 0$ ), the equation simplifies to the following expression



The current flowing in an electrochemical cell can be a result of two processes: faradaic or nonfaradaic. A faradaic process involves the transfer of electrons across the electrolyte-electrode interface, like the reactions previously discussed. Nonfaradaic processes do not transfer electrons, such as adsorption and desorption of ions or double-layer (capacitive) charging. Hence, Faraday's law cannot be applied to these processes.

The potential applied to a cell or an electrode can drive a reaction to occur if the voltage is sufficient. However, a portion of the applied potential is devoted to overcoming resistances, the most significant often being solution resistance. This loss of or drop in applied voltage is referred to as ohmic or IR drop and can be calculated with Ohm's law:

$$E = IR_s \quad (2.4)$$

If the ohmic drop is uncompensated and significant, then it can introduce errors in measurements and analysis.

## 2.2. Thermodynamics

Thermodynamics provides information concerning the possibility of a certain reaction or phase formation. Typically, the spontaneity of a reaction is determined using the change in Gibbs free energy ( $\Delta G$ ) which can be calculated as follows:

$$\Delta G = \Delta G^{\circ} + RT \ln(Q) \quad (2.5)$$

where  $Q$  is the reaction quotient which is the product of the activity of products raised to their stoichiometric coefficient divided by the product of the activity of the reactants raised to their stoichiometric coefficient. In electrochemistry, a reaction typically involves oxidation or reduction via electron transfer. If (2.5) is adapted for (2.3), it becomes the following equation

$$\Delta G = \Delta G^o + RT \ln \left( \frac{a_{M^{p+}}}{a_{M^{n+}}} \right) \quad (2.6)$$

The activity of an electron in a metal “can be disregarded because the electron concentration never changes appreciably” (52).

In electrochemistry, it is more convenient to work with potential ( $E$ ) than  $\Delta G$ . The reversible (infinite resistance) potential is related to  $\Delta G$  by the charge passed, as shown below

$$\Delta G = -nFE \quad (2.7)$$

The negative sign is due to the electrochemical convention that a positive potential corresponds to a spontaneous process. Combining (2.6) and (2.7) results in the *Nernst* equation:

$$E = E^o - \frac{RT}{nF} \ln \left( \frac{a_{M^{p+}}}{a_{M^{n+}}} \right) \quad (2.8)$$

The potential obtained with this equation can be considered the equilibrium potential or open-circuit (i.e.,  $I = 0$ ) potential of a redox reaction. The activity can be defined by (2.9) and (2.10)

$$a = \gamma x \quad (2.9)$$

$$a = \gamma_c \frac{C}{C^o} \quad (2.10)$$

If  $p = 0$  in (2.8) and the reduced metal does not interact with the electrode or another reduced metal, then its activity can be assumed to be one. However, if multiple metals are deposited and form an alloy, then activity cannot be assumed to be one. In molten salt electrochemistry, (2.9) is prevalently used.  $C^o$  is the concentration at which the standard reduction potential ( $E^o$ ) is defined which is commonly 1 molal (53). It is common for the activity coefficient to be grouped with  $E^o$  to form the apparent or formal standard reduction potential ( $E^{o'}$ )

$$E^{o'} = E^o - \frac{RT}{nF} \ln \left( \frac{\gamma_{M^{p+}}}{\gamma_{M^{n+}}} \right) \quad (2.11)$$

Thus,  $E^{o'}$  is only constant if the activity coefficients do not depend strongly on composition over the concentration range of interest. Again, if  $p = 0$ , then activity coefficient is assumed to be unity unless an intermetallic forms in the deposit.

### 2.3. Reaction Kinetics

For a single-step, elementary reaction, its net rate is given by the resulting law as applied to (2.3)

$$r = k_f C_{M^{n+}} - k_b C_{M^{p+}} \quad (2.12)$$

Rate constants are known to have an Arrhenius relationship with temperature and activation energy

$$k = Ae^{-\frac{E_a}{RT}} \quad (2.13)$$

If the reaction is occurring in a condensed phase, then activation energy can be related to a “standard Gibb’s free energy of activation” (52) which can be related to potential, as

expressed in (2.14) and (2.15)

$$k_f = k^o \exp \left[ -\frac{\alpha n F}{RT} (E - E^{o'}) \right] \quad (2.14)$$

$$k_b = k^o \exp \left[ \frac{(1 - \alpha) n F}{RT} (E - E^{o'}) \right] \quad (2.15)$$

The transfer coefficient ( $\alpha$ ) accounts for the amount of the potential that promotes the reduction (forward) reaction. The standard rate constant ( $k^o$ ) is the forward and backward rate constants at equilibrium under the special conditions that  $E = E^{o'}$  and the bulk concentrations are equal ( $C_{M^{n+}}^b = C_{M^{p+}}^b$ ). If (2.14) and (2.15) are substituted into (2.12) and Faraday's law is applied ( $I = nFAr$ ), then the faradaic current related to the reaction in (2.3) is given by (2.16)

$$I = nFAk^o \left( C_{M^{n+}} \exp \left[ -\frac{\alpha n F}{RT} (E - E^{o'}) \right] - C_{M^{p+}} \exp \left[ \frac{(1 - \alpha) n F}{RT} (E - E^{o'}) \right] \right) \quad (2.16)$$

This expression is very useful, but can be expressed more conveniently. This is done by introducing a term called the exchange current density ( $i_o$ ). This is derived by evaluating (2.16) at equilibrium (i.e.,  $I = 0$ ) and results in the equation below

$$i_o = nFAk^o \left( C_{M^{n+}}^b \right)^{1-\alpha} \left( C_{M^{p+}}^b \right)^{\alpha} \quad (2.17)$$

Substituting (2.17) into (2.16) and multiplying by negative one yields the *current-overpotential* relationship in the IUPAC convention (53)

$$I = i_o \left( \frac{C_{M^{p+}}}{C_{M^{n+}}^b} \exp \left[ \frac{(1 - \alpha) n F}{RT} \eta \right] - \frac{C_{M^{n+}}}{C_{M^{p+}}^b} \exp \left[ -\frac{\alpha n F}{RT} \eta \right] \right) \quad (2.18)$$

If the surface and bulk concentrations are assumed to be equal, (2.18) simplifies to the more common *Butler-Volmer* equation. The overpotential ( $\eta$ ) is defined as the offset of

potential from the equilibrium potential

$$\eta = E - E^{o'} + \frac{RT}{nF} \ln \left( \frac{C_{M^{p+}}^b}{C_{M^{n+}}^b} \right) \quad (2.19)$$

### 2.3.1. Metal Electrodeposition Kinetics

In the case of  $p = 0$ , a metal is deposited onto the electrode. In this case, the concentration of reduced metal ( $C_M$ ) becomes a common term in the derived kinetic expressions because most literature assumes that the reduced product is soluble when deriving kinetic expressions. However, this can be confusing because most metals are insoluble in molten salts and other electrolytes. Various methods of handling the deposited metal concentration have been proposed when deriving the kinetic expressions. The simplest approach is to assume that the bulk and surface concentration of the deposited metal are the same (54). Another option is to use the standard concentration as a “scaling concentration” (55). However, the first approach only resolves the problem in a few situations and neither approach may hold when two metals deposit and alloy with each other. A more general, albeit more complicated, approach derives an alternative current-overpotential relation by starting with a slightly different rate law (56):

$$R = k_f a_{M^{n+}} - k_b a_M \quad (2.20)$$

By following the same steps in the previous derivation in Section 2.3, this modification of the *current-overpotential* relation is derived in the American or polarographic convention (56):

$$I = i_o \left( \frac{a_{M^{n+}}}{a_{M^{n+}}^b} \exp \left[ -\frac{\alpha nF}{RT} \eta \right] - \frac{a_M}{a_M^b} \exp \left[ \frac{(1-\alpha) nF}{RT} \eta \right] \right) \quad (2.21)$$

where the modified definitions of  $i_o$  and  $\eta$  are given in (2.22) and (2.23).

$$i_o = nFAk^o \left(a_{M^{n+}}^b\right)^{1-\alpha} \left(a_M^b\right)^\alpha \quad (2.22)$$

$$\eta = E - E^o + \frac{RT}{nF} \ln \left( \frac{a_M^b}{a_{M^{n+}}^b} \right) \quad (2.23)$$

In this case, activity of the metal deposits can be assumed to be one if the metal deposits are pure. This assumption is not valid when less than a monolayer of a metal is deposited on a foreign substrate or when two metals deposit and interact to form a metallic solution. In such cases, the activity of the metals would need to be determined for (2.21) to be applied. A simple model for activity of a monolayer of metal is that the activity of the metal is proportional to the fraction of the electrode surface covered by the metal (52)

$$a_M = \frac{\gamma_M A_M}{A} \quad (2.24)$$

However, this ignores nucleation effects which are common for deposited metals. For co-deposition of two metals, this would require significant study of the metal-metal interactions under the electrochemical cell conditions to determine the activities of metals.

## 2.4. Mass Transport

The kinetic expressions in (2.18) and (2.21) have two separate terms for concentrations or activity in the bulk and at the electrode surface illustrating that the conditions are different at the surface of an electrode than in the bulk solution. These differences are the result of mass transport mechanisms, namely diffusion, convection, and migration. All of these mechanisms are encapsulated in the flux ( $j$ ) of an ion.

The flux is driven by the difference in the electrochemical potential ( $\bar{\mu}$ ) which is related to the chemical potential ( $\mu$ ).



$$\bar{\mu} = \mu^o + RT \ln(a) + nF\phi \quad (2.25)$$

The last term accounts for electrical properties of the ion's environment and is related to the charge of the ion and absolute potential ( $\phi$ ) of the ion's location. Ions in a solution will move or generate a flux to relieve gradients in the electrochemical potential. Thus molar flux can be calculated from the gradient of electrochemical potential and any convective flow

$$j = -\frac{CD}{RT} \nabla \bar{\mu} + Cv \quad (2.26)$$

Substituting (2.25) into (2.26) yields this general equation

$$j = -CD \nabla \ln(a) - CD \frac{nF}{RT} \nabla \phi + Cv \quad (2.27)$$

By introducing a few assumptions to (2.27), it simplifies to the *Nernst-Planck* equation

$$j = -D \frac{dC}{dx} - CD \frac{nF}{RT} \frac{d\phi}{dx} + Cv \quad (2.28)$$

The assumptions in (2.28) include one-dimensional transport and the equivalence of activity and concentration. The three terms in equations (2.27) and (2.28) represent first diffusion, then migration, and lastly convection. Using Faraday's law ( $I = nFAj$ ), the flux can be related to current.

In certain cases, flux equations can be simplified by neglecting migration, convection or both. The convection term can be neglected in stagnant fluids. The migration term is less significant at low currents due to a weaker electric field (i.e., lower overpotentials). The addition of a supporting (i.e., not electroactive) electrolyte can almost completely remove migration effects. Supporting electrolytes can also reduce the effects of ohmic drop in the solution. If the convection and migration terms are neglected,

then the Nernst-Planck equation reduces to Fick's first law

$$j = -D \frac{dC}{dx} \quad (2.29)$$

Fick's second law is derived from the first law and is the origin of almost every electroanalytical expression derivation

$$\frac{dC}{dt} = D \frac{d^2C}{dx^2} \quad (2.30)$$

Thus, it should be noted that derived electroanalytical expressions in the next section apply the assumption of a stagnant fluid and negligible migration unless otherwise noted.

## 2.5. Electroanalytical Methods

Electroanalytical methods are techniques that investigate the behavior of an ion of interest called an analyte by manipulating potential or current and measuring the other. Four terms are frequently used when describing electroanalytical techniques: amperometry, potentiometry, voltammetry, and coulometry. Amperometry controls the potential, usually holding it steady at one setting, and measures the current. It can be considered a subclass of voltammetry. Potentiometry measures potential while controlling the current. Voltammetry, like amperometry, measures current and controls potential, but voltammetric techniques involve more than fixing the potential at a set value. It can include scanning the potential or a series of potential steps with a certain pattern. Coulometry measures the charge under potential controlled conditions and can affect the bulk characteristics of the electrochemical solution. The first three techniques are carried out under small A/V conditions meaning that the area of the electrode is small enough that the current passed does not alter the properties of bulk volume. Coulometric techniques can pass sufficient current to alter the conditions in the bulk solution.

As discussed in Section 1.4, the techniques of interest in this project are chronoamperometry (CA), cyclic voltammetry (CV), open-circuit potentiometry (OCP) and normal pulse voltammetry (NPV). The derivations of key relations for each of the listed techniques are reviewed in this section along with key assumptions. These methods involve applying a waveform and measuring the response which can typically be described by a derived equation. A summary of each technique is provided in Table 2.1.

### 2.5.1. Chronoamperometry

CA involves stepping the potential from an initial potential level at which no faradaic current flows to a potential at which faradaic current flows and is diffusion-limited. The diffusion-limited current can be determined by solving Fick's second law with the accompanying boundary conditions

$$\frac{dC_{M^{n+}}}{dt} = D_{M^{n+}} \frac{d^2 C_{M^{n+}}}{dx^2} \quad (2.31)$$

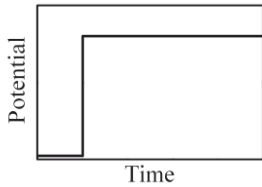
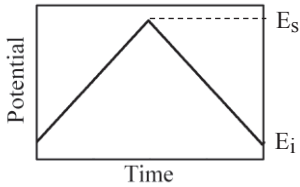
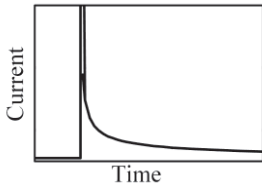
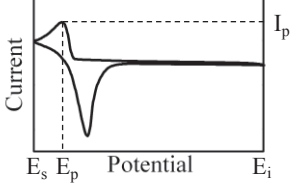
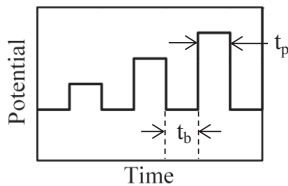
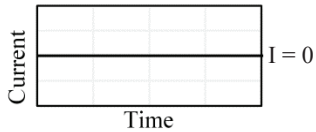
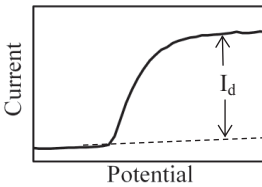
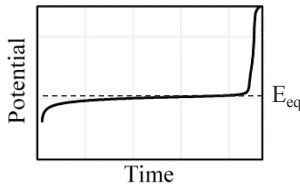
$$C_{M^{n+}}(x, 0) = C_{M^{n+}}^b \quad (2.32)$$

$$\lim_{x \rightarrow \infty} C_{M^{n+}}(x, t) = C_{M^{n+}}^b \quad (2.33)$$

$$C_{M^{n+}}(0, t) = 0 \quad (2.34)$$

From (2.31), it is evident that one-dimensional semi-infinite linear diffusion is assumed. Also, the diffusion coefficient is assumed to be spatially independent and, therefore, independent of concentration, because concentration is varying with location as demonstrated by the boundary conditions, (2.33) and (2.34). The time, at which the potential is stepped, is considered zero (i.e.,  $t = 0$ ) and no faradaic current is flowing. Thus, metal ions are uniformly distributed throughout the solution as indicated by the

Table 2.1 Summary of electroanalytical methods

	Chronoamperometry (CA)	Cyclic Voltammetry (CV)
Waveform		
Response		
Key Equations	$I(t) = nFA \sqrt{\frac{D}{\pi t}} C$	$I_p = 0.6105A \sqrt{\frac{(nF)^3 D v}{RT}} C$
	Normal Pulse Voltammetry (NPV)	Open-Circuit Potentiometry (OCP)
Waveform		
Response		
Key Equations	$I_d = nFA \sqrt{\frac{D}{\pi t_p}} C$	$E_{eq} = E^{o'} + \frac{RT}{nF} \ln \left( \frac{x_o}{x_R} \right)$

initial condition, (2.32). After the potential is stepped, the concentration of metal ions in the bulk solution is unaffected, if the small A/V conditions hold. If the potential step is large enough, the metal ions at the surface will be immediately and completely reduced resulting in diffusion controlling the rate of reduction.

The solution to (2.31) is obtained by using Laplace transforms and the initial and boundary conditions which results in a temporal concentration profile. The concentration profile can be differentiated and substituted into Fick's first law which can be related to current by Faraday's law. This results in the *Cottrell* equation

$$I(t) = nFAC_{M^{n+}}^b \sqrt{\frac{D_{M^{n+}}}{\pi t}} \quad (2.35)$$

According to the equation, the current approaches infinity at very short times and zero at very long times. However, in practice, this is not observed. At longer times, natural convection can prevent the current from completely decaying away. For metal electrodeposition, the area can also increase substantially which can cause the current to depart from Cottrellian behavior. On a short timescale, limitations in the equipment can prevent measurement and recording of very large currents. Additionally, double layer charging can significantly distort the current signal at very short times.

To illustrate these important limitations and considerations, a CA measurement as part of the experiments in this work (mixture D6) is displayed in Figure 2.1 along with the current predicted by the Cottrell equation. Initially, it can be seen that the potentiostat and its software is unable to capture the high current predicted by the Cottrell equation. Then after 1 s, the magnitude of the current ceases to decay and actually grows. This is due to the growth of metal deposits on the WE, which increases its surface area.

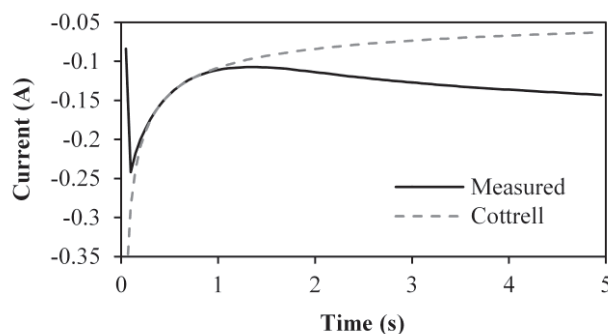


Figure 2.1 Chronoamperogram at  $E = -2.08$  V vs Ag/AgCl(1 wt%) for mixture D6 (4.69 wt%  $\text{GdCl}_3$ , 2.45 wt%  $\text{LaCl}_3$ ,  $T = 500^\circ\text{C}$ , Area =  $0.35 \text{ cm}^2$ )

### 2.5.1.1 Double-Layer Charging

The interfaces between the electrode and solution tend to behave as capacitors due to excess charges in the vicinity of the interface. When the interface is perturbed from its initial state, significant amount of the current is consumed by the nonfaradaic process of charging the double layer. For a potential step, the resulting charging current is given by the following expression

$$I(t) = \frac{\Delta E}{R_s} e^{-t/R_s C_d} \quad (2.36)$$

The change in potential or the size of the potential step is represented by  $\Delta E$ . The product of  $R_s$  and  $C_d$  is commonly referred to as the time constant. Until the time is equivalent to 5 time constants, the current due to double layer charging cannot be neglected.

The eutectic LiCl-KCl salt has been found to have a resistance from 0.4-2  $\Omega/\text{cm}$  depending on the analytes present and their concentration based on published results (57–60). Additionally, the reported capacitance of the double layer in molten LiCl-KCl is 0.1-2.0  $\text{mF}/\text{cm}^2$  (57,59). The absolute resistance for a particular setup depends upon the distance between the RE and WE. The absolute capacitance depends on the surface area of the WE. Two approaches to reduce the effect of capacitive current are, first, to sample

the current at sufficiently long time that capacitive currents can be neglected and second, to design your cell to reduce the time constant for capacitive currents. Table 2.2 shows the variation of the  $R_s C_d$  (RC) time constant with WE and RE spacing and WE surface area, if the largest values of  $2 \Omega/\text{cm}$  and  $2.0 \text{ mF}/\text{cm}^2$  are assumed for a conservative estimate of the RC time constant. It should be noted that the reduction of the RC time constant has practical limitations. For example, too close of spacing could cause shorting when metal deposits form on the WE or inhibit diffusion of ions to the WE surface.

### 2.5.1.2 Semi-Infinite Linear Diffusion

Cylindrical electrodes are commonly used for electrochemical measurements in molten LiCl-KCl eutectic. If the cylindrical electrode is small enough radially or the current is sampled for a short enough time, then the semi-infinite linear diffusion assumption may introduce significant error. To illustrate the possible error that could be introduced by assuming linear diffusion at cylindrical electrodes, the current response for CA was calculated for diffusion at a planar electrode using (2.35) and at a cylindrical electrode at various diameters using the following approximation which is accurate within 1.3% (52)

Table 2.2 Variation of the time constant (in ms) with electrode spacing and WE area

		Surface Area ( $\text{cm}^2$ )				
		0.2	0.4	0.6	0.8	1
Electrode Spacing (cm)	0.2	0.2	0.3	0.5	0.6	0.8
	0.4	0.3	0.6	1.0	1.3	1.6
	0.6	0.5	1.0	1.4	1.9	2.4
	0.8	0.6	1.3	1.9	2.6	3.2
	1	0.8	1.6	2.4	3.2	4.0

$$I = \frac{nFADC}{r_o} \left[ \frac{2 \exp(-0.05 \sqrt{4\pi Dt}/r_o)}{\sqrt{4\pi Dt}/r_o} + \frac{1}{\ln(5.2945 + 0.7493 \sqrt{4\pi Dt}/r_o)} \right] \quad (2.37)$$

The calculated current responses for planar and cylindrical diffusion at the WE with a diameter of 0.5 mm are plotted in Figure 2.2. Initially, the current responses are identical. However, at longer times, the current responses diverge. Thus, if the current was measured using a 0.5 mm WE and sampled at 1 s, but analyzed using the Cottrell equation, which assumes planar diffusion, the current would be underestimated by about 10%. This would in turn overestimate the concentration of ions in the molten salt by 11%. As shown in Figure 2.3, the error can be reduced by sampling at shorter times or using a cylindrical WE with a larger diameter. This could also be resolved by using the same diameter WE for measuring the diffusion coefficients and determining concentrations which would effectively embed the error in the diffusion coefficient.

Further analysis of Figure 2.2 reveals another approach that could minimize the error introduced by using cylindrical WE. If the current is plotted versus the inverse of the square root of time, then the slope would be proportional to concentration according to the Cottrell equation. The slopes of both curves are nearly identical (<0.001%) in Table 2.3. Practically, all of the difference between the curves is found in the y-intercept.

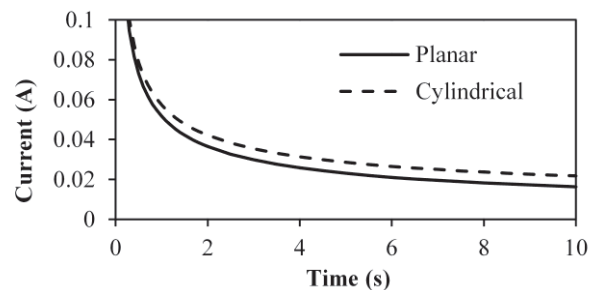


Figure 2.2 Calculated current response with planar and cylindrical diffusion for CA



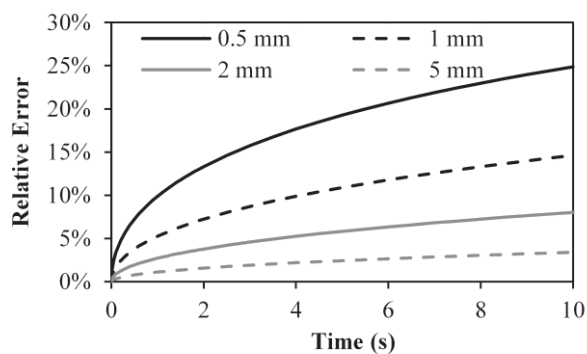


Figure 2.3 Relative error of the calculated current at a cylindrical WE of various diameters (0.5-5 mm) as a function of sampling time

Table 2.3 Comparison of the regressions of current with  $t^{-1/2}$

Planar		Cylindrical	
Slope	Y-int	Slope	Y-int
0.051642	0	0.051643	0.005713

### 2.5.2. Cyclic Voltammetry

The general concept of CV is to scan the potential over a range of potential values at a certain rate and measure the current response. As the potential reaches values at which species in the solution or on the electrode will react, the changes in the current are measured accordingly. When the maximum or minimum potential is reached the direction of the scan is reversed creating a cycle of the potential. A closely related technique called linear sweep voltammetry (LSV) simply scans in one direction and terminates when the end potential is reached.

By scanning the potential, a wealth of information is obtained about the system. However, to extract meaningful quantitative information from CV, the analysis can become extensive and complex. The derivations of key analytical expressions and their assumptions are dependent on the standard rate constant of an ion ( $k^o$ ), the scan rate ( $\nu$ )

and solubility of the reduced species in the electrolyte. The parameter,  $\Lambda$ , which is the ratio of intrinsic reaction rate to mass transfer rate, is often used to determine whether the reaction is reversible, quasi-reversible or irreversible, as shown in Table 2.4. Thus, reversible processes are characterized by fast reaction kinetics relative to mass transfer, and irreversible processes are characterized by slow reaction kinetics relative to mass transfer. Quasi-reversible processes are in between the two extreme conditions and use certain functions/profiles to blend the reversible and irreversible functions. This classification of reversibility is specific to electrochemistry and should not be confused with *chemical* reversibility. In fact, this kind of reversibility is frequently referred to as *electrochemical* reversibility/irreversibility.

Once a system has been properly identified, the appropriate equations can be applied to characterize the properties of the ions or determine concentrations. These equations are summarized in Table 2.5. The derivations, assumptions, characteristics and application of these functions are discussed in the following sections.

### 2.5.2.1 Reversible

The listed conditions for determining the type of CV define reversibility by the speed of the electron transfer process relative to the scan rate ( $\nu$ ) of the potential. The rationale is that if electron transfer is fast, then equilibrium is achieved rapidly and can be assumed at the electrode surface. In such a case, the Nernst equation can be applied

Table 2.4 Criteria for Reversibility, Quasi-reversibility and Irreversibility (61)

Reaction Type	Dimensionless	For T=773 K, D=10 <sup>-5</sup> cm <sup>2</sup> /s, $\alpha=0.5$
Reversible	$\Lambda > 15$	$k^o > 0.32\sqrt{n\nu}$ cm/s
Quasi-Reversible	$15 > \Lambda > 10^{-2(1+\alpha)}$	$0.32\sqrt{n\nu} > k^o > 2.12 \times 10^{-5}\sqrt{n\nu}$ cm/s
Irreversible	$\Lambda < 10^{-2(1+\alpha)}$	$k^o < 2.12 \times 10^{-5}\sqrt{n\nu}$ cm/s

Table 2.5 Summary of expressions used for CV

Reversible (soluble-soluble) (63)	Reversible (soluble-insoluble) (64)
<i>Randles-Sevcik</i>	<i>Berzins-Delahay</i>
$I_p = 0.4463A \sqrt{\frac{(nF)^3 D_o v}{RT}} C$	$I_p = 0.6105A \sqrt{\frac{(nF)^3 D_o v}{RT}} C$
$E_p = E^{o'} + \frac{RT}{nF} \ln \left( \sqrt{\frac{D_R}{D_o}} \right) - 1.109 \frac{RT}{nF}$	$E_p = E^{o'} + \frac{RT}{nF} \ln(x_o) - 0.854 \frac{RT}{nF}$
$\Delta E_p =  E_p - E_{p/2}  = 2.20 \frac{RT}{nF}$	$\Delta E_p =  E_p - E_{p/2}  = 0.774 \frac{RT}{nF}$
Quasi-Reversible (soluble-soluble) (61)	Irreversible (soluble)* (65)
<i>Delahay</i>	<i>Delahay</i>
$\Lambda = \frac{k^o}{\sqrt{D_o^{1-\alpha} D_R^\alpha \frac{nFv}{RT}}}$	$I_p = 0.4958nFA \sqrt{\frac{\alpha nF D_o v}{RT}} C$
$I_p = I_p(rev) K(\Lambda, \alpha)$	
$E_p = E^{o'} + \frac{RT}{nF} \ln \left( \sqrt{\frac{D_R}{D_o}} \right) - \Xi(\Lambda, \alpha) \frac{RT}{nF}$	$E_p = E^{o'} + \frac{1}{b} \left( 0.780 + \ln \left( \frac{\sqrt{D_o b v}}{k^o} \right) \right) b = \frac{\alpha nF}{RT}$
$\Delta E_p =  E_p - E_{p/2}  = \Delta(\Lambda, \alpha) \frac{RT}{nF}$	$\Delta E_p =  E_p - E_{p/2}  = 1.857 \frac{RT}{\alpha nF}$
* An irreversible peak assumes that the potentials are such that anodic processes are negligible	

$$E = E^{o'} - \frac{RT}{nF} \ln \left( \frac{C_{M^{p+}}}{C_{M^{n+}}} \right) \quad (2.38)$$

This version of the Nernst equation uses the concentration convention for activity and the standard apparent potential which includes the activity coefficients. The potential in this case is also a function of time

$$E = E_i - vt \quad (2.39)$$

For simplicity only the LSV potential function is included here. The CV function only varies slightly and has been demonstrated elsewhere (62). The steps and assumptions are identical with only the modified CV function of potential inserted.

**2.5.2.1.1 Soluble product.** A potential scan can be thought of as a series of

infinitesimally small potential steps. Hence, (2.31)–(2.33) are applied for the oxidized species. The last boundary condition, (2.34), is not applied because the small potential steps do not necessarily produce complete diffusion control. Instead, another boundary condition is formulated by substituting (2.39) into (2.38) resulting in an equation that can relate the oxidized and reduced species to one another as a function of time.

Another difference is that the flux of the reduced species needs to be considered, because the overpotential may not be large enough to neglect it. Thus, boundary conditions for the reduced species are similar to the oxidized species, except that the bulk concentration of the reduced species is replaced by zero, if it is initially absent. The sum of the flux of the oxidized and reduced species is then set equal to zero

$$D_{M^{n+}} \frac{dC_{M^{n+}}}{dx} + D_{M^{p+}} \frac{dC_{M^{p+}}}{dx} = 0 \quad (2.40)$$

This is solved using Laplace transforms and results in a function whose maximum (i.e., peak current) can be characterized by the *Randles-Sevcik* equation (62,63)

$$I_p = 0.4463 A \sqrt{\frac{(nF)^3 D_{M^{n+}} \nu}{RT}} C_{M^{n+}} \quad (2.41)$$

**2.5.2.1.2 Insoluble product.** However, if the product is a deposited metal which is insoluble in the solution, there is no flux due to the reduced species which alters the solution. Since no reduced species is present in the solution, (2.40) is replaced by (2.31). The initial condition and first boundary condition are (2.32) and (2.33) respectively. The second boundary condition is formulated from a modified form of (2.38)

$$E = E^{o'} + \frac{RT}{nF} \ln(C_{M^{n+}}) \quad (2.42)$$

(2.39) is substituted into (2.42) and solved for  $C_{M^{n+}}$  to formulate the second boundary

condition. Again, Laplace transforms are performed to obtain an equation that describes the reduction peak of the oxidized metal ion. The peak current of the resulting function is described by the *Berzins-Delahay* equation (64)

$$I_p = 0.6105 A \sqrt{\frac{(nF)^3 D_{M^{n+}} \nu}{RT}} C_{M^{n+}} \quad (2.43)$$

Both for soluble and insoluble, the Nernst equation is invoked to generate the needed boundary conditions. Thus, it is assumed that the potential is scanned at a slow enough rate to allow equilibrium to be achieved at the electrode surface. If  $k^o$  is large, this can be achieved at high scan rates. Inevitably, as scan rate increases, the assumption of equilibrium at the WE surface will become invalid. This is well demonstrated by  $\text{UCl}_3$  in LiCl-KCl eutectic, as shown in Figure 2.4 which plots the peak current versus the square root of scan rate from mixture N1 (see Section 3.3.2 and Appendix A for more details). Initially, the peak current is linear with the square root of scan rate, as predicted by (2.41) and (2.43). However, between 0.2 and 0.3 V/s, the peak begins to depart from the linear trend, this is most likely due to the transition from reversibility to quasi-reversibility (59,66,67). As a result, the peak heights are lower. Thus the limits of reversibility and irreversibility need to be known and well understood so that the correct equations are applied to determine concentrations.

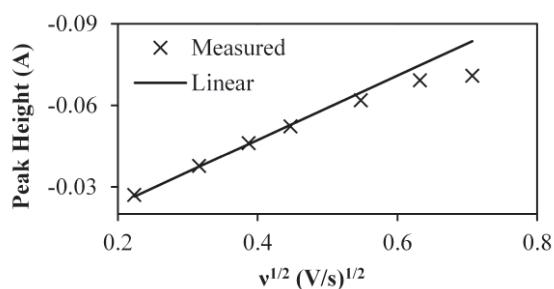


Figure 2.4 Plot of  $\text{U}^{3+}$  reduction peak height versus square root of scan rate for mixture N1 (0.83 wt%  $\text{UCl}_3$ , WE Area =  $0.73 \text{ cm}^2$ ,  $T = 500^\circ\text{C}$ )

Linearity of peak height with scan rate is insufficient to deduce reversibility. As seen in Table 2.5, reversible and irreversible expressions are proportional to the square root of scan rate. The unique feature of electrochemical reversibility is the independence of peak potential ( $E_p$ ) with scan rate. The half-peak width ( $\Delta E_p$ ) can also be used to determine reversibility, irreversibility, or quasi-reversibility. However, at these potentials, a significant amount of current could be flowing which may require compensation for ohmic drop to accurately diagnose the reversibility of the system. Thus (2.4) must be applied to determine the contribution of resistance to the potential at the WE. Once quantified, that amount needs to be subtracted from the observed or applied peak potential to obtain the accurate peak potential value.

Neglecting to account for ohmic drop may result in mischaracterizing the reaction mechanism, as demonstrated for mixture N1 in Figure 2.5, which plots the peak potential of  $\text{UCl}_3$  in  $\text{LiCl-KCl}$  at different scan rate with and without accounting for ohmic drop. The resistance of the salt was measured to be  $0.3 \, \Omega$  using the current interrupt method. When the potential is not adjusted for ohmic drop, it appears that the peak potential is a function of scan rate. However, if the adjustment is made, peak potential has almost no

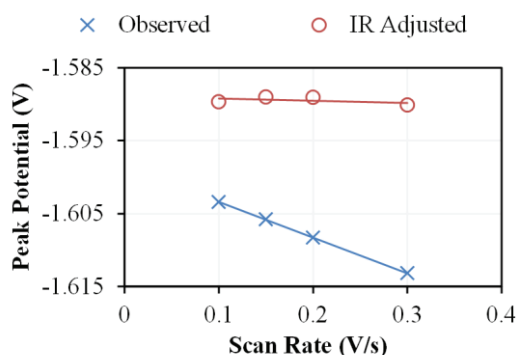


Figure 2.5 Peak potential of  $\text{U}^{3+}$  with and without adjustment for ohmic (IR) drop for mixture N1

trend with scan rate. This adjustment is also required in order to obtain accurate  $E^{o'}$  values from the peak potential.

#### 2.5.2.2 Quasi-Reversible

Quasi-reversible peaks are the most difficult to analyze. The analysis essentially attempts to characterize the peak by blending the reversible and irreversible functions in Table 2.5 by using the  $K$ ,  $\mathcal{E}$ , and  $\Delta$  functions or profiles, which are available in literature (52,61). These profiles were derived by solving (2.40) with same initial and boundary conditions that were used for the reversible and soluble product CV case with the exception that the Nernst equation cannot be applied. Instead the flux is equated to reaction rate as derived in (2.16). This results in the following expression

$$D_{M^{n+}} \frac{dC_{M^{n+}}}{dx} = k^o \left( C_{M^{n+}} \exp \left[ -\frac{\alpha nF}{RT} (E - E^{o'}) \right] - C_M \exp \left[ \frac{(1-\alpha)nF}{RT} (E - E^{o'}) \right] \right) \quad (2.44)$$

By solving (2.40) with the new boundary condition, Masuda and Ayabe (61) showed that the peak shape was a function of  $\alpha$  and a parameter,  $\Lambda$

$$\Lambda = \frac{k^o}{\sqrt{D_o^{1-\alpha} D_R^\alpha \frac{nFv}{RT}}} \quad (2.45)$$

As seen in Table 2.5, the  $K$ ,  $\mathcal{E}$ , and  $\Delta$  functions depend on  $\alpha$  and  $\Lambda$ . Unfortunately, only limited work has been done on quasi-reversible systems that involve an insoluble product. Only the anodic dissolution peak has been characterized, because the deposition peak is complicated by nucleation which inhibited the application of the expression derived by Avaca (55) for quasi-reversible electrodeposition. Unfortunately, the anodic peak for metal dissolution is not as repeatable as the cathodic peak since it depends on the potential at which the CV was reversed and the morphology of the metal deposit. Thus,

the applicability of the quasi-reversible equations in Table 2.5 is questionable for the soluble-insoluble reaction.

By examining the properties of the  $K$  function, which is a scaling function for peak current, some insight can be gained into its applicability to soluble-insoluble systems. At sufficiently low scan rates,  $K$  is equal to one and constant making the peak current function equivalent to the reversible expression. At a sufficiently high scan rate,  $K$  is equal to a constant value which depends on the value of  $\alpha$  so that the resulting peak current expression is equivalent to the irreversible case. Essentially, at high scan rates,  $K$  is the ratio of the irreversible over the reversible peak function. By comparing the reversible and irreversible equations in Table 2.5, it can be seen that the only variations in the peak current expression are the leading constants and the  $\alpha$  term in the irreversible expression. Thus, a constant ratio results if the irreversible expression is divided by the reversible expressions which results in 0.78 for soluble-soluble reactions and 0.57 for soluble-insoluble reactions, if  $\alpha = 0.5$ . Hence, theoretically,  $K$  function will not result in the irreversible expression if applied to the Berzins-Delahay equation.

This theoretical exercise can be verified using experimental data. Marsden and Pesic (68) studied cerium electrodeposition and plotted the peak height for the reduction of  $\text{Ce}^{3+}$  to Ce metal versus the square root of scan rate from a very low scan rate ( $\sim 5$  mV/s) to a very high scan rate ( $\sim 1.5$  V/s) at 653 K. This plot is reprinted here in Figure 2.6 in which the peak current clearly transitions from one linear curve to another linear curve as the scan rate increases. They explained that this is “characteristic of a quasi-reversible system where the system displays Nernstian behavior at low scan rates but transitions to irreversibility at high scan rates” (68). They also calculated that at 653 K,



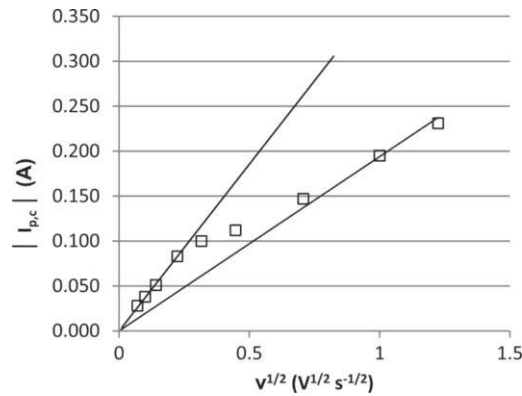


Figure 2.6 Reduction peak height of  $Ce^{3+}$  as a function of the square root of scan rate (Figure 5 in original work) (68). Reproduced by permission of The Electrochemical Society.

$\alpha = 0.48$ . Thus, the slope at high scan rates (irreversible region) divide by the slope at low scan rates (reversible region), should be close to 0.78 for the  $K$  function to apply.

The slopes of the reversible and irreversible lines were determined to be 0.369 and 0.193 respectively, by digitizing the two lines in Figure 2.6. This results in a ratio of 0.52 which is much closer to 0.57 calculated earlier. Thus, it appears that the  $K$  function is inapplicable to soluble-insoluble reactions in theory and practice.

### 2.5.2.3 Irreversible

The irreversible system is simplified by the assumption that the backward reaction is negligible reducing (2.44) to the following expression

$$D_{M^{n+}} \frac{dC_{M^{n+}}}{dx} = k^o \left( C_{M^{n+}} \exp \left[ -\frac{\alpha n F}{RT} (E - E^{o'}) \right] \right) \quad (2.46)$$

The same problem is solved, (2.40), with the same boundary and initial conditions, as was done for the quasi-reversible process with the exception that (2.46) is used instead of (2.44). The benefit of irreversible peaks is that kinetic information can be calculated. As seen in Table 2.5, the kinetic parameters,  $\alpha$  and  $k_o$ , are found in the expressions for

irreversible CV peaks. In addition to those expressions, another equation for the peak current can be derived in terms of the peak potential, as shown below

$$I_p = 0.227nFAC_{M^{n+}}k_o \exp\left[-\frac{\alpha nF}{RT}(E_p - E^{o'})\right] \quad (2.47)$$

Thus, a plot of the  $\ln(I_p)$  versus  $E_p - E^{o'}$  should yield a linear plot with a slope and an intercept proportional to  $\alpha n$  and  $k_o$ , respectively.

### 2.5.3. Normal Pulse Voltammetry

Since the waveform for NPV is more complex than other techniques, it is reprinted and enlarged in Figure 2.7 for convenience. NPV is essentially a series of CA tests with a “rest” time in between during which no species is electroactive with exception of reduced species reoxidizing. This is particularly important for metal electrodeposition at nonpolarographic (i.e., nonrenewing) electrodes. By holding the potential for an extended period of time ( $t_b$ ) at a base potential ( $E_b$ ) sufficiently positive, the deposited metal can reoxidize and the nonpolarographic electrode can return to its original state. However, not only does the electrode surface need to be allowed to return to its original state, the diffusion layer needs to as well. Otherwise, an accumulation or depletion of ions in the diffusion layer could cause the magnitude for the diffusion-limited current ( $I_d$ ) to be artificially increased or decreased. In the case of depletion, the

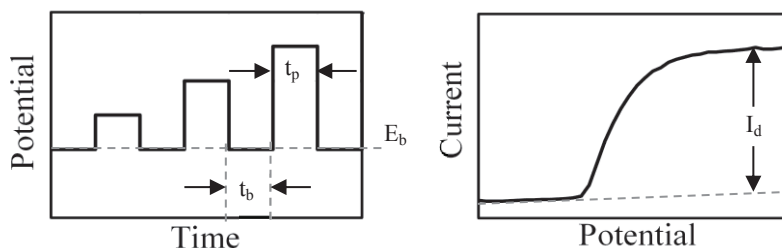


Figure 2.7 Enlargement of NPV waveform (left) and response (right) from Table 2.1

curve takes on a peak shape, like in CV. In some cases, the time required to renew the conditions near and at the electrode can require more than 10 s, resulting in a much slower turnaround time for NPV (>10 min) than for CV (<1 min).

After renewing the electrode surface and diffusion layer, the potential is pulsed into the region where the species of interest are electroactive for a short amount of time ( $t_p$ ), and the current is sampled at the end of the pulse. Because this is a potential step method, all of the considerations and limitations discussed for sampling CA also apply here. Thus,  $t_p$  should be long enough that nonfaradaic currents do not significantly contribute, but should also be short enough that electrode area does not increase.

The measured response for NPV is on the right in Figure 2.7 and plateaus when the current is diffusion limited.  $I_d$  is directly proportional to concentration as predicted by the Cottrell equation, (2.35), except that  $t$  is replaced by  $t_p$ .

#### 2.5.4. Open-Circuit Potentiometry

OCP is facilitated by the Nernst equation, (2.8). Thus equilibrium conditions need to be imposed (i.e., zero current) while the potential is measured. Either the mole fraction or molar concentration convention can be used. It may be advantageous to remain in the molar concentration convention, since all the other methods were derived based on the molar concentration convention. In the case of metal deposition, some metal needs to be initially present on the electrode in order to record its open-circuit potential with its ion. This could be done by using an electrode made of the metal of interest or by pre-depositing some metal on an inert electrode, then enforcing an open-circuit. The measured potential at open-circuit should vary logarithmically with concentration or mole fraction. If this behavior can be verified for molten salt mixtures of interest, then it could

be used to determine concentration.

#### 2.5.4.1 Reference Electrode Conversions

When applying the OCP method, there is a logarithmic relation between concentration and measured potential. This approach to concentration measurement can be highly sensitive to small errors in experimental setup or analysis approach. For example, the conversion between reference electrode potentials can be critical, but there is inconsistency in the literature regarding that conversion. The potential at a  $\text{Cl}^-/\text{Cl}_2(1 \text{ atm})$  electrode, the standard chlorine electrode (SCE), is the de facto reference potential that can be directly related to standard free energy of formation. But it is impractical to use such an electrode as the reference. Alternatively, an Ag/AgCl reference electrode is a popular choice for molten chloride systems. But to compare studies on the same basis and calculate activity coefficients, the potential of such an Ag/AgCl reference electrode must be converted to the SCE scale. The potential of an Ag/AgCl electrode depends upon the concentration of AgCl in the RE. Thus, in most works, the potentials measured versus an Ag/AgCl RE are converted to the SCE potential. In literature there are a couple formulas and data sets for converting from the Ag/AgCl to the SCE. Unfortunately, they are inconsistent as shown in Table 2.6.

Table 2.6 Potential difference from Ag/AgCl to SCE

Source	1 wt% (0.39 mol%)	1 mol%	5 mol %
Yang-Hudson (69)	-1.223	-1.167	-1.071
Shirai et. al. (70)	-1.073	-1.017	-0.921
Shirai et. al.*	-1.182	-1.119	-1.012
Mottot (71)	-1.368	-1.305	-1.198
Lantelme-Berghoute (58)	-1.201	---	-1.049
*Corrected for sharp density increase near 100 mol% AgCl			

The Yang-Hudson reference measured the potential of the Ag/AgCl potential experimentally against a SCE and is commonly cited in published experimental studies of ions in molten LiCl-KCl eutectic. Shirai et al. (70) performed similar work to Yang-Hudson, but measured significantly different potential values under similar conditions. However, when extrapolated with respect to molarity as opposed to mol% to account for the density variations, their value for  $E^{o'}$  produced results more consistent with Yang-Hudson. An expression derived by Mottot has also been used and is quite different from the other sources. The Lantelme-Berghoute reference measured the reduction potentials of  $\text{La}^{3+}$  and  $\text{Gd}^{3+}$  ions directly with a SCE. The reduction potentials of these ions were measured by the author using a 1 wt% and 5 mol% AgCl RE. The values reported in the last row of Table 2.6 are the calculated difference between the measured and reported values by Lantelme and Berghoute which agree well with the Yang-Hudson reference.

Such large variation in reported potentials is problematic. This could indicate that small changes in experimental conditions could drastically affect the recorded potential values. To demonstrate the impact of small potential variations, a hypothetical situation is proposed. If a  $E^{o'}$  value is converted to the SCE using the Yang-Hudson data by an author, then it will need to be converted back to the Ag/AgCl scale to be applied to an open-circuit potential measured versus Ag/AgCl RE. However, if the factor used to convert  $E^{o'}$  is inconsistent, off calibration or the potential of the RE has slightly shifted, then the concentration determined from the open-circuit potential could be quite inaccurate. In this case, the error relative to the Yang-Hudson source introduced by inconsistent conversion values are reported in Table 2.7, but a shift in the RE potential would have the same effect. The errors are quite large even when the conversion factors

Table 2.7 Effect of RE conversion on mol% measurement

Source	Shirai et. al.	Shirai et al.*	Mottot	Lantelme-Berghoute
Relative Error	86000%	1300%	-100%	169%

used only varied by tens of millivolts. Thus, if OCP is to be employed as a concentration measurement technique a highly stable RE needs to be employed.

## 2.6. Summary

This chapter has reviewed the known fundamental theory of electrochemical kinetics, transport, and thermodynamics from literature and has discussed its application to the study of electrodeposition of metal, which is the main subject of interest for this thesis. Derived equations for electroanalytical techniques have been reviewed, examining their assumptions and applicability to electrodeposition. It is essential to examine the measured data to ensure that assumptions applied are consistent across all data sets and concentrations and with the method employed (i.e., CA, CV, etc.); otherwise, variations in data will be manifested that are unrelated to concentration variations. This could skew calibration curves or alter diffusion coefficient values. Thus, before calculating key parameters or constructing calibration curves, certain checks have been revealed to be necessary from examining the assumptions of the electrochemical methods. The checks, equations, and theory will be applied and referenced in Chapters 5-7 in which electrochemical data is analyzed.

### 2.6.1. Chronoamperometry

The key assumption in CA is that semi-infinite linear diffusion limits the process. Diffusion limitation can be checked by overlaying the temporal current profile measured

at various potentials. When the profiles overlap, then the process is confirmed to be diffusion limited since the Cottrell equation is independent of potential. The semi-infinite linear diffusion assumption can introduce error into this work since cylindrical electrodes are used for the WE. Thus, the diameter of WE was held constant within each test matrix to standardize the error.

### 2.6.2. Cyclic Voltammetry

Key characteristics of CVs vary with scan rate resulting in three categories: (1) reversible, (2) quasi-reversible, and (3) irreversible. Plotting the peak height versus the square root of scan rate can be used to identify transitions from reversibility to quasi-reversibility or from quasi-reversibility to irreversibility. Linear trends of peak height with the square root of scan rate indicate either a reversible or irreversible region. The CVs need to be further classified by analyzing the trend of peak potential with scan rate. If the peak potential is independent of scan rate then reversibility can be concluded, otherwise the system is irreversible. Since expressions for quasi-reversible soluble-insoluble cyclic voltammetry have not successfully been derived and derivation of such expression is beyond the scope of this dissertation, the quasi-reversible region is avoided.

### 2.6.3. Normal Pulse Voltammetry

The key to NPV is the assumption that the WE surface and diffusion layer has been restored to the original state. The main inhibitor to the renewal of the WE surface is persistent metal deposits. If significant deposits accumulate the NPV signal will not plateau, but continually increase. The depletion of ions is most likely to be cause of non-renewal of the diffusion layer since it is conducted in stagnant media. This would be

indicated by the current slightly decreasing at more extreme potentials. Thus, these phenomena are observed, the base time will be increased, to the extent possible, which will allow more time for the renewal of the WE surface or diffusion layer.

#### 2.6.4. Open-Circuit Potentiometry

OCP measurements are subject to shifts in potentials due to drift over time or differences in the composition of AgCl in the REs used. To check the consistency of the RE potential, the potential of lithium ion deposition and/or dissolution of the WE will be used. These values should be consistent because their bulk properties change very little from one experiment to another.

It is clear from examining the theory that the behavior of ions at each concentration needs to be determined to avoid introducing variances in the data unrelated to concentration. Thus, in addition concentration measurements, the analyses and verification methods discussed will also be performed as part of the results when clear boundaries between signals are discernable.

In addition to the theory or electrochemistry, some limited practical considerations have been mentioned for applying electrochemistry to molten salt cells. The next chapter covers in more detail the practicalities of designing and performing electrochemical experiments in molten salts. Furthermore, the application of the electroanalytical theory discussed in this chapter on multi-analyte mixtures depends upon good separation of the signals. The method of separating the signals is particular to analyte pairings and is discussed in the chapters relevant to the pairing results.